

Automated Glass Fragmentation Analysis

Gaile G. Gordon
TASC
55 Walkers Brook Drive
Reading, MA 01867
gggordon@tasc.com

ABSTRACT

This paper describes a novel automated inspection process for tempered safety glass. The system is geared toward the European Community (EC) import regulations which are based on fragment count and dimensions in a fractured glass sample. The automation of this test presents two key challenges: image acquisition, and robust particle segmentation. The image acquisition must perform well both for clear and opaque glass. Opaque regions of glass are common in the American auto industry due to painted styling or adhesives (e.g. defroster cables). The system presented uses a multiple light source, reflected light imaging technique, rather than transmitted light imaging which is often used in manual versions of this inspection test. Segmentation of the glass fragments in the resulting images must produce clean and completely connected crack lines in order to compute the correct particle count. Processing must be therefore be robust with respect to noise in the imaging process such as dust and glint on the glass. The system presented takes advantage of mathematical morphology algorithms, in particular the watershed algorithm, to perform robust preprocessing and segmentation. Example images and image segmentation results are shown for tempered safety glass which has been painted on the outside edges for styling purposes.

Keywords: segmentation, morphology, inspection, fracture analysis

1 BACKGROUND AND INTRODUCTION

Fragmentation testing is an integral part of the European Community (EC) regulations addressing quality control for automotive tempered safety glass.¹ The EC glass fragmentation standards are based on localized particle count and dimension criteria, and present many challenges for automation. As a result, EC fragmentation testing is typically performed manually. The manual process is both time consuming and error prone. In contrast, the equivalent United States (US) regulations² are based primarily on the weight of the largest fragment. The US tests are routinely automated via mechanical filtering and scales. In this paper, we describe a novel *automated* visual inspection process developed at TASC which addresses the EC glass fragmentation standards.

The automation of the fragmentation test presents several key technical challenges. The first is the image acquisition. Transmitted light techniques, which are currently used for the manual inspection process, are not effective for imaging cracks in opaque regions of the glass. Opaque glass, due to paint or adhesives (e.g. defroster cables) is occurring more and more frequently in the American auto industry (see Figure 1). The second issue is effective automated segmentation

of the cracked glass images. During the analysis of the images each crack line must be cleanly identified, and the cracks surrounding each glass fragment must be completely connected. Noise in the imaging process or cracks which are aligned with the line of sight often result in incomplete or missing crack lines.

More background on the fragmentation regulations and the current manual inspection process are provided in the following section 1.1. Solutions for image acquisition of clear and opaque cracked glass are presented in section 2. The segmentation algorithm developed is described in detail in section 3.

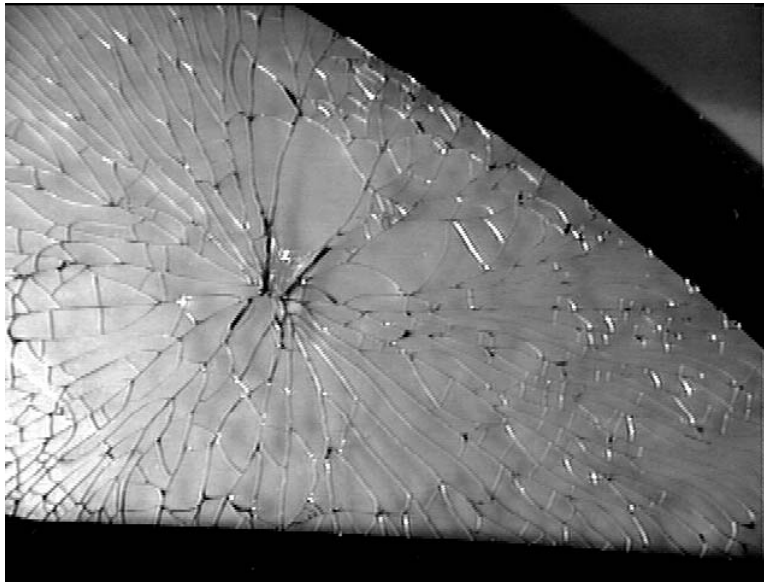


Figure 1: Fractured rear side window panel containing clear and opaque glass. Edges of glass have been painted for styling purposes.

1.1 Fragmentation Testing

The most common way to evaluate the effectiveness of tempered safety glass is to break the glass and observe the fracturing behavior. If the processing is flawed, the size of the resulting fragments will be too large or they will be irregularly shaped. The timing of the test is important because the glass will continue to break for some time after the initial fracture. The EC fragmentation tests require a photographic contact print be made (and archived) of the broken glass panel between 10 seconds and 3 minutes after initial fracture. Because the size of the glass panels can be large, blue print paper is often used for contact printing.

Based on evaluation of the crack lines in the contact print, the number of particles in any $5\text{cm} \times 5\text{cm}$ region must be between certain limits, typically 40 and 400. Because this regulation is based on localized regions, the glass particles must remain in the correct relative position after fracture. This is usually achieved by placing an adhesive film on the glass before it is broken. Additional considerations apart from localized particle count are also of interest, including maximum particle area and maximum particle extent.

This test is performed each production run, sometimes up to twice per shift on each line depending on the quantity of glass manufactured. A medium sized manufacturing facility might perform a fragmentation test every 20 minutes based on these requirements.

Particle counting is currently done manually, by choosing several areas on the contact print which appear to represent the

largest range of particle size. A contact print will always be 1:1 with respect to the scale of the original glass. Therefore, the average particle size for a $5\text{cm} \times 5\text{cm}$ region with 400 particles is 6.25mm , or 2.5mm on a side for a square fragment. The relatively poor quality of the blue print image and potentially small particle size makes manual counting of the fragments very difficult. Figure 2 clearly demonstrates the difficulty even for medium to large particle sizes. This figure shows a section from an actual blue print style contact print marked with a $5\text{cm} \times 5\text{cm}$ grid. The target region has approximately 125 fragments. It is not hard to imagine that this counting method is tedious, error prone, and time consuming.

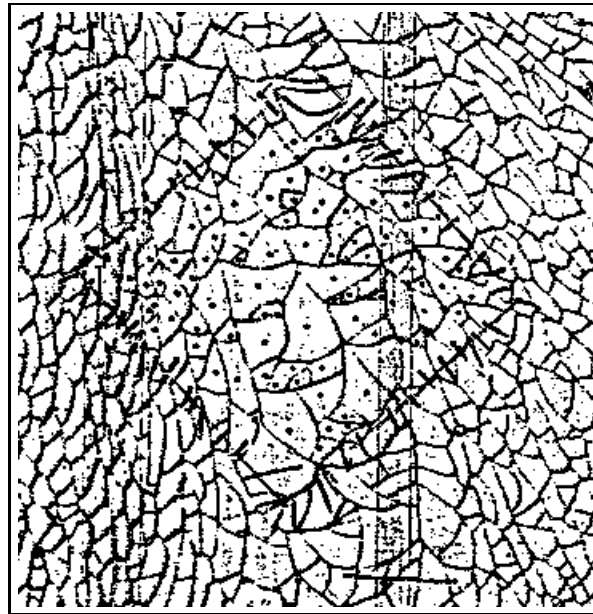


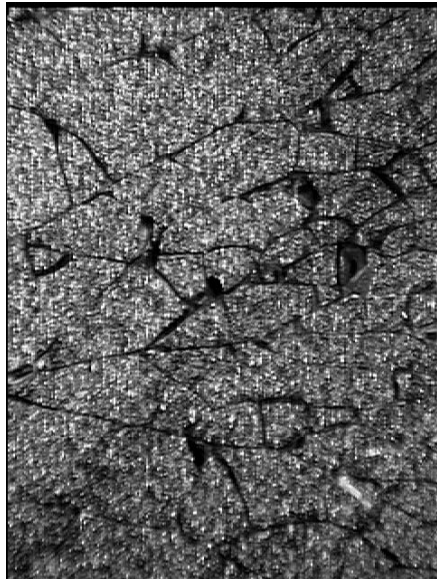
Figure 2: Section of a blue print contact including a $5\text{cm} \times 5\text{cm}$ grid for manual counting of particles. Vertical lines are caused by the edges of adjacent pieces of transparent adhesive used to maintain the relative position of the fragments after fracture.

2 IMAGING CRACKED GLASS PANELS

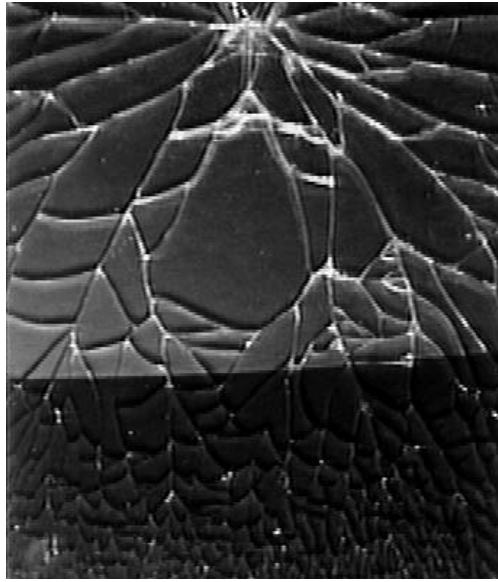
Contact print methods record light intensity transmitted through the glass. Crack lines image darker than unbroken clear glass. Since painted regions of the glass are common in the American automotive industry, we will continue to use paint as an example when discussing opaque glass. Painted regions attenuate the light to a large degree and the patterns of the paint itself interfere with detection of the crack lines. This is demonstrated by Figure 3(A) which shows a transmitted light image taken with a very bright light source. Crack lines are still not clearly visible in many portions of the image.

An important aspect of opaque adhesives such as paint, defroster cables, and antenna wires is that they are applied to only one side of the glass. By imaging the glass from the clear side using reflected light techniques, the cracks are detectable even if the other side of the glass is completely impenetrable to light. Figure 3(B) shows an example of a glass panel with both clear and painted regions which has been placed on a black surface. The light source is oblique to the surface of the glass and crack lines or, more specifically, the shadows of the crack lines are visible in both regions of the glass.

Lighting becomes an important variable when using reflected light techniques. We are imaging the crack lines indirectly by observing their shadows, so any crack line which is aligned with the light direction will not be easily detected. For this reason, two images are taken, each with a single oblique light source. The two light source directions are separated by 90° . Figure 4 shows examples of this technique. Cracks which are difficult to detect in one image are clear in the other image. The two images will be combined during the processing to produce a single coherent record of crack lines. Scattered white glint spots visible in these images are from glass dust generated in the initial fracture.



(A)



(B)

Figure 3: (A) Transmitted light image of cracks in a painted region. (B) Reflected light image of cracks in glass containing clear and opaque regions.

3 SEGMENTATION ALGORITHMS

The goal of the inspection process is to count the particles in a given region and provide statistics on particle size and dimension. This is achieved by identifying and completing the crack lines imaged and then computing the bounds of each fragment. The result of this process is an image which attaches to each pixel an identifier or label indicating the fragment to which it belongs. This image can be used to quickly count the unique labels (fragments) within a given region as well as to compute minimum and maximum area and maximum extent of for all fragments.

There are several steps in the segmentation process:

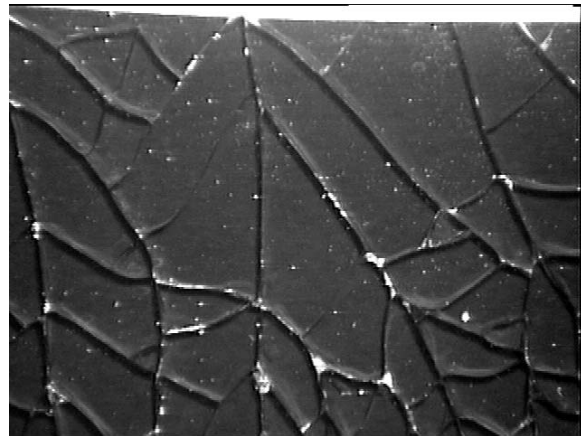
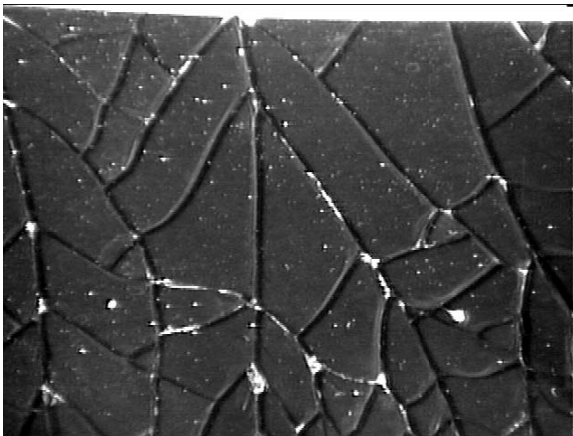


Figure 4: Reflected light images of opaque glass region with two different light source directions.

- Preprocessing to remove image noise
- Independent segmentation of crack lines for both light directions
- Refinement of crack lines: thinning and connecting crack boundaries
- Identification and labeling of particles

Each step is described in detail in the following sections.

3.1 Preprocessing

As Figure 5(A) shows, there are a variety of types of noise in the original crack images. The bright glint noise is caused by glass dust or the crack edges themselves. The dark noise is due either to dirt on the glass or shadows of glass dust. In the preprocessing stage, each image is filtered individually to remove both white glint noise and isolated black spots using some common morphological operators.^{3,4}

The bright noise is either in isolated areas, or next to the crack lines. A two step process eliminates both while minimizing change to crack lines. First, bright outliers (2 standard deviations or more above the mean intensity) are replaced with dark outliers (value 2 standard deviations below the mean) which approximate the intensity level of the crack lines, see Figure 5(B). Next, a morphological opening with an octagonal structuring element is performed to remove the smaller remaining bright noise. This is shown in Figure 5(C). The last step is to eliminate isolated dark spots without eliminating the dark lines of similar thickness. This is done by taking the minimum of closings with 4 different orientations of linear structuring elements.⁵ The final result is shown in Figure 5(D).

3.2 Initial Binary Crack Segmentation

After noise elimination, the next step is to segment each image approximately into regions of background and crack lines. The background is always locally lighter than the crack shadows, but a simple threshold would not segment the image effectively because the light level varies across the image. A better approach is to approximate the background, and subtract the original image from the background image. A simple threshold of the difference image will produce a more consistent result. The background is estimated using a closing of the original image with an octagonal structuring element larger than the width of the crack lines. This common segmentation process is often called *valley detection* or more specifically the inverse *top hat transform*.⁶ These results of these steps are shown in Figure 6(A) and (B) for the two different light source directions.

The results of each of the independent binary segmentations are combined to produce a single image with a more complete representation of the crack lines. This is achieved by taking the maximum value from the two images at each pixel. As is seen in Figure 6(C), there is a gap along many parts of the crack lines because we have been detecting shadow lines, not the crack lines themselves. This gap is filled using a closing with a small structuring element. The final result after some additional clean up of small area components is shown in Figure 6(D). The crack lines are thickened, but by using multiple light directions, representations of all crack edges are present.

3.3 Crack Refinement

When tempered glass fractures, the particles take on generally convex shapes. We can take advantage of this observation to complete crack lines which may not have been completely detected. Another more traditional method might be to complete lines by bridging gaps of a certain size locally, e.g. dilation followed by constrained skeletonization, as was done

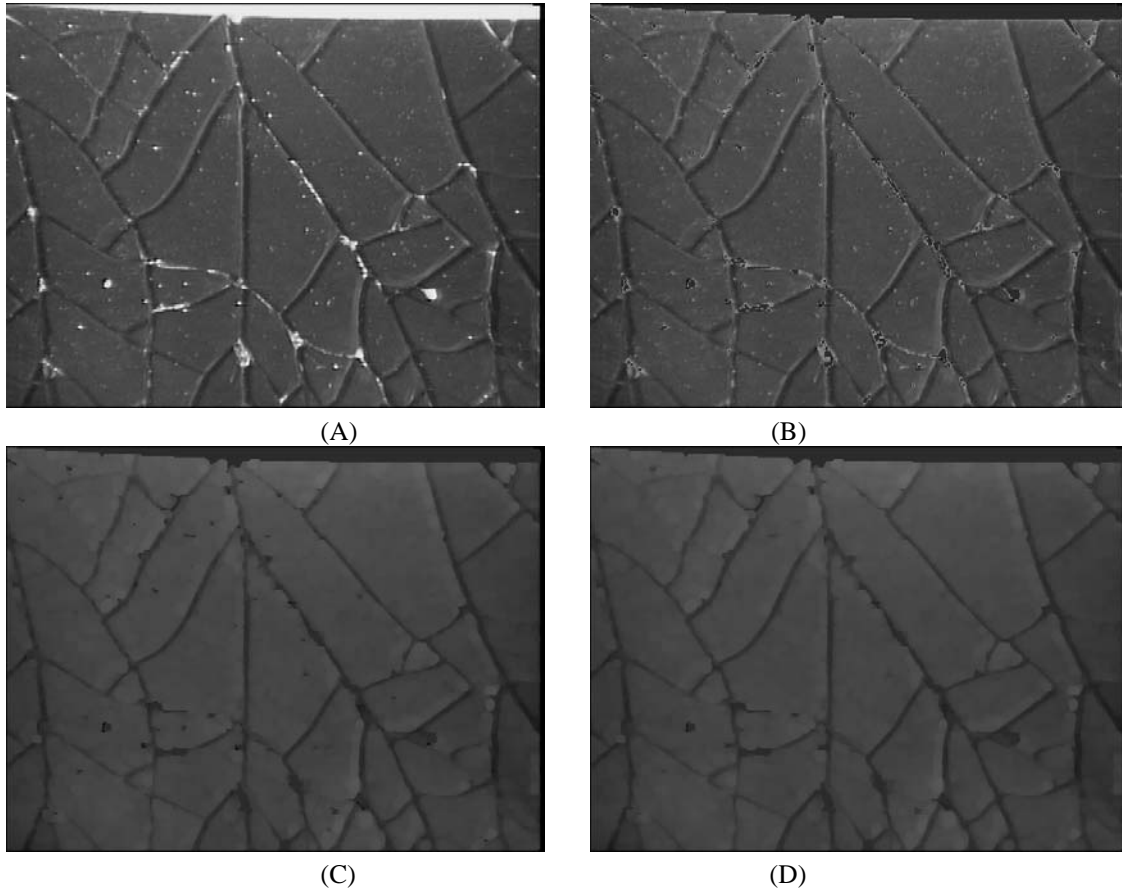


Figure 5: Elimination of noise: (A) Original, (B) replace high outliers with low outliers, (C) opening with octagonal structuring element, and (D) minimum of closings with linear elements at 0, 45, 90, 135 degree orientations.

in.⁷ But by taking advantage of domain knowledge provided by the convexity criterion, this process can be performed more robustly.

The determination of convexity is made using the distance transform. We measure the distance at each point not on a crack line to the nearest crack line pixel given by the binary segmentation. In a convex particle, there will be a single point (or several connected points) in the middle of a particle which has the maximal distance for that particle. For concave particles, however, there will be multiple maxima. So the regional maxima of the distance transform can be used to mark each convex glass fragment. The distances are approximated in the traditional 2 pass sequential algorithm.^{8,9} Details of this calculation, including a mechanism for indicating a degree of tolerated concavity, are given below.

If only the count of the particles is necessary, the process would be complete after the location of the regional maxima of the distance transform. However, to compute the area and dimensional statistics, the crack lines themselves must be found as well. This is done by considering the inverse distance function as a topographic relief. The crack lines are located at the watershed boundaries of this “terrain”.

In terms of real physical terrain, the watershed line follows ridge lines which divide adjacent drainage areas. Rain falling on opposite sides of a watershed line will eventually collect in different drainage basins. The watershed algorithm used here^{10,11} simulates a progressive flooding of the relief “by immersion”. Imagine the local minima of the relief are “punctured” and the terrain is lowered progressively into a body of water. The water level will rise, and eventually neighboring basins will merge, signaling the existence of a watershed division. These merge points are recorded. When the terrain is completely

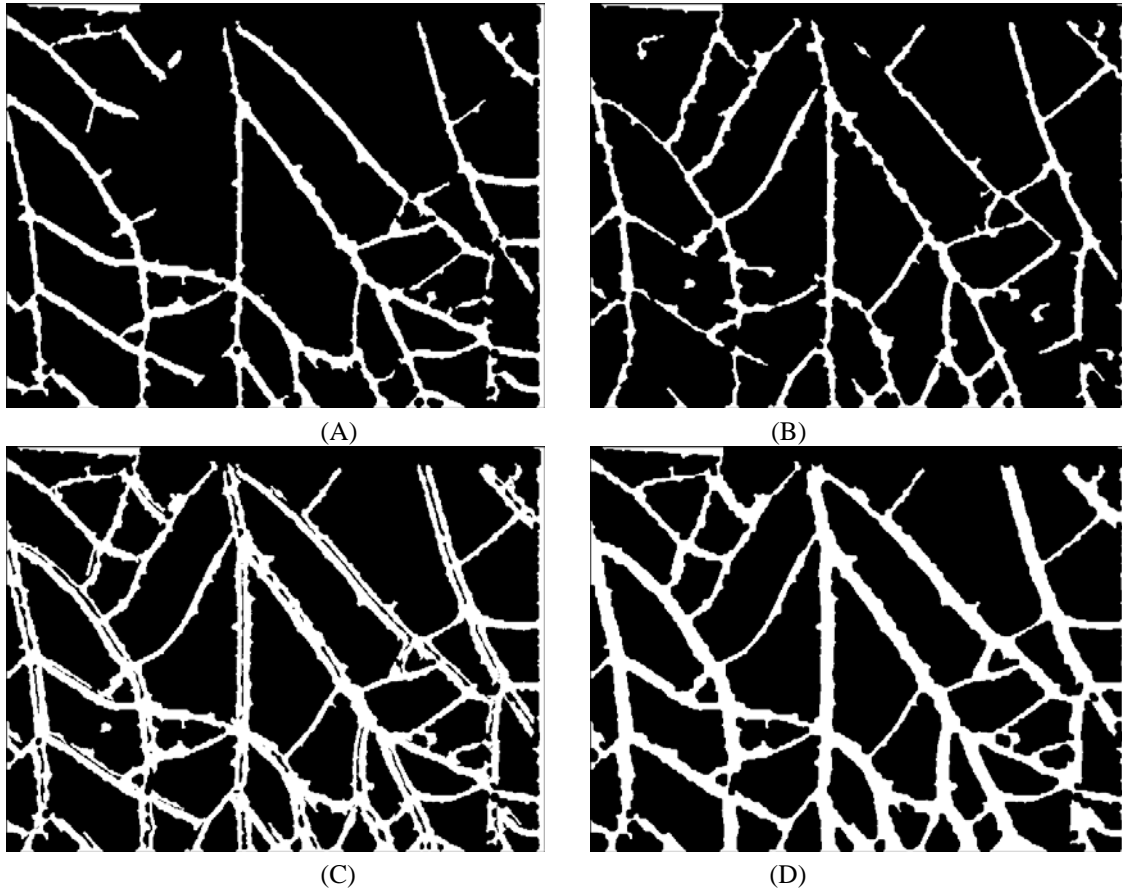


Figure 6: Initial crack segmentation: (A)(B) Independent segmentation of two images, (C) combined results, and (D) final merged result.

flooded the watershed lines will be completely connected around each initial local minimum. The starting point for the watershed is the set of uniquely labeled markers already computed.

Implementation Details and Examples

In practice, some mildly concave shapes will be produced during fracture and our initial binary segmentation has noisy edges which would cause over segmentation if the convex requirement were observed strictly. There must be some mechanism to provide a level of concavity to be allowed in the segmentation.

This tolerance is provided by flattening the peaks of each maximum in the original distance function to $P_i - T$, where P_i is the original height, and T is a constant tolerance. Since each peak is at a potentially different height, this is done by greyscale reconstruction of the distance function from the difference image (distance - T).¹² Figure 7(A) shows the result of this operation with $T = 5$. Note that the peaks have become plateaus. This flattening will have the effect of joining peaks separated in height by T or less. The resulting maximal plateaus are shown in Figure 7(B).

The computed watershed lines are shown overlaid on one of the original images in Figure 8(A). The fragments themselves are then differentiated and highlighted in Figure 8(B) as with a connected component algorithm.¹³ The number of distinct component labels detected in a subimage provides a direct measure of the number of particles in that region. Some

adjustment is made for particles which intersect the boundaries of the region. The EC regulations specify that boundary particles are counted as a half particle. Equivalently, the number of pixels labeled with a unique label provides a good estimate of the area of that particle. Therefore, a simple local image histogram on a subimage of the component image completes the fragment analysis process.

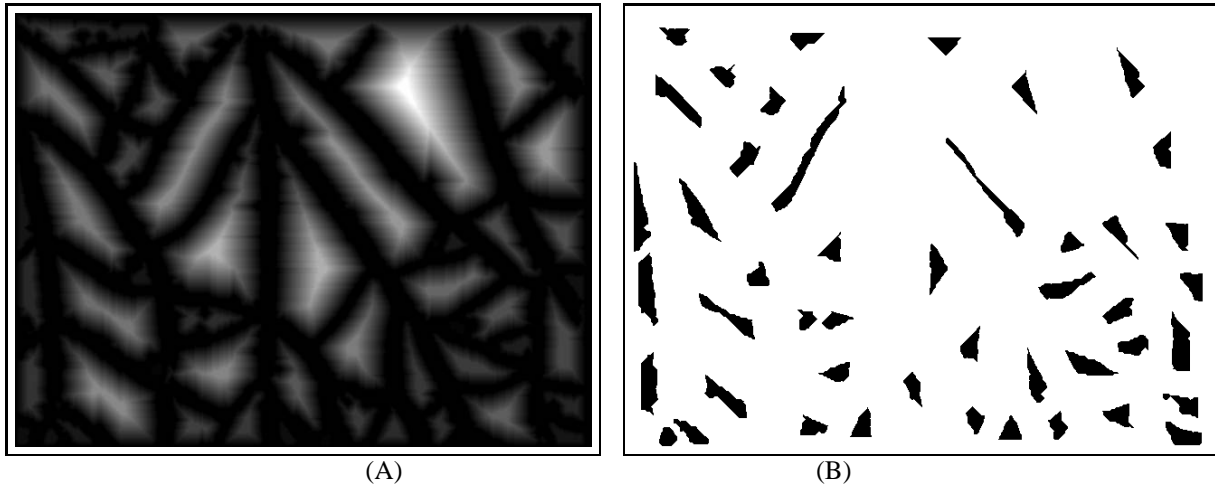


Figure 7: (A) Modified distance function: grayscale reconstruction of distance function from the difference image (distance - T) for $T = 5$, (B) Maximal regions which provide markers for each fragment.

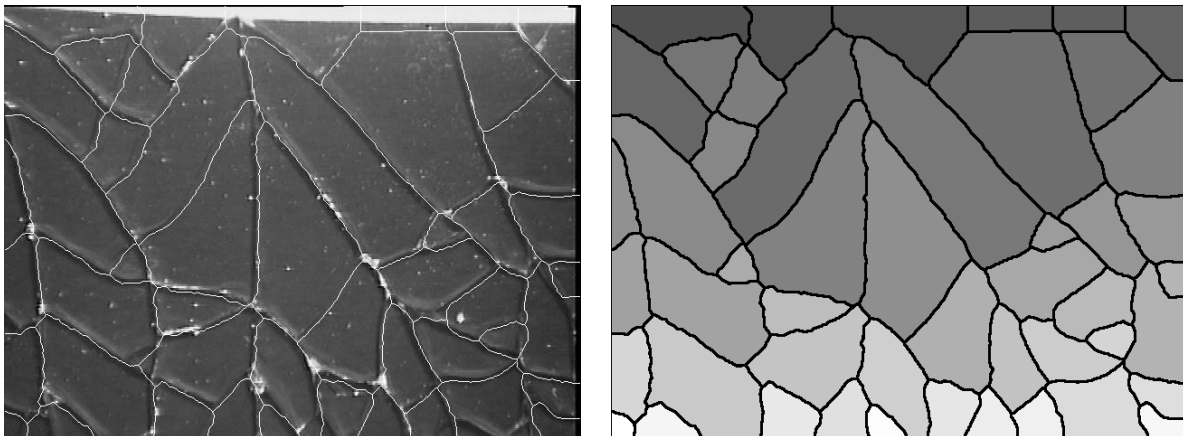


Figure 8: (A) Crack line segmentation shown in white overlaid on one of the original images, (B) Individual fragments are identified and labeled with a unique color.

4 SUMMARY

The problem of automated fragmentation analysis for EC inspection of auto safety glass is challenging because it is highly visually oriented and requires localized fragment counts instead of the global statistics on which US requirements are based. TASC has implemented a successful processing system which includes imaging techniques effective for both clear and opaque regions of glass. This paper presents successful automated analysis techniques resulting in clean particle segmentation from which fragment statistics are computed including local particle counts and overall extremes in particle area.

5 REFERENCES

- [1] E/ECE, *Agreement concerning the Adoption of Uniform Conditions of Approval and Reciprocal Recognition of Approval for Motor Vehicle Equipment and Parts. Addendum 42, Regulation No. 43: Uniform Provisions Concerning the Approval of Safety Glazing and Glazing Material, Annex 5*, February 1988.
- [2] *ANSI Z26.1*, 1983.
- [3] J. Serra, *Image Analysis and Mathematical Morphology*. London: Academic Press, 1982.
- [4] J. Serra, ed., *Image Analysis and Mathematical Morphology, Volume 2: Theoretical Advances*. London: Academic Press, 1988.
- [5] J. Serra and L. Vincent, "An overview of morphological filtering," *Circuits, Systems and Signal Processing*, vol. 11, pp. 47–108, Jan. 1992.
- [6] F. Meyer, "Contrast feature extraction," in *Quantitative Analysis of Microstructures in Material Sciences, Biology and Medicine*, (J.-L. Chermant, ed.), (Stuttgart, FRG), Riederer Verlag, 1978. Special issue of Practical Metallography.
- [7] G. G. Gordon, "Face recognition from depth maps and surface curvature," in *Proceedings of SPIE Conference on Geometric Methods in Computer Vision*, (San Diego, CA), July 1991.
- [8] A. Rosenfeld and J. Pfaltz, "Distance functions on digital pictures," *Pattern Recognition*, vol. 1, pp. 33–61, 1968.
- [9] G. Borgefors, "Distance transformations in digital images," *Computer Vision, Graphics, and Image Processing*, vol. 34, pp. 334–371, 1986.
- [10] L. Vincent and P. Soille, "Watersheds in digital spaces: an efficient algorithm based on immersion simulations," *IEEE Transactions on Pattern Analysis and Machine Intelligence*, vol. 13, pp. 583–598, June 1991.
- [11] L. Vincent and E. R. Dougherty, "Morphological segmentation for textures and particles," in *Digital Image Processing Methods*, (E. R. Dougherty, ed.), pp. 43–102, New York: Marcel-Dekker, 1994.
- [12] L. Vincent, "Morphological grayscale reconstruction in image analysis: Applications and efficient algorithms," *IEEE Transactions on Image Processing*, vol. 2, pp. 176–201, Apr. 1993.
- [13] A. Rosenfeld and A. C. Kak, *Digital Picture Processing, Second Edition*. Vol. 2, Orlando, Florida: Academic Press, Inc., 1982.